Journal of Mobile Multimedia, Vol.3, No.3 (2007) 255-264

BATHYMETRIC FORECASTING USING MULTILAYER SPATIAL IMAGES

PETRUS PARYONO

Duta Wacana Christian University, Yogyakarta
petrus@ukdw.ac.id, pparyono@yahoo.com

Received March 13, 2007
Revised June 21, 2007

Earth-observing satellite, such Landsat, provide many multitemporal images of earth surface, either water body or land. By using spectral water body characteristics and field measurement, the bathymetry (water depth) of the study area can be derived from images recorded/acquired at different times. In this study, four multitemporal spatial images were used for generating bathymetry images which were arranged as multilayer images in cubic raster database format. Bathymetric forecasting is needed for a dynamic (rapidly change) area, such as an estuary of a river transporting a lot of sediments. Bathymetric forecasting in this study area utilized linear and quadratic regressions techniques. The spatial image layers representing standard errors values, constants of linear and quadratic equations were generated from the cubic raster database containing multitemporal images. These layers were also arranged in a cubic raster database format. By visual observation on image of standard error, a user may analyse which part of the study area that close to the field reality and which part that does not. The values of each layers were then classified into several classes and were displayed using distinctive colors to ease the user in visual observation. The bathymetric forecasting (either forward or backward) can be calculated from the spatial linear and quadratic equations. In order to provide more impressive visualization, the time series of bathymetric images generated were compiled into one file in animated gif format.

Key words: Spatial image, cubic raster database, bathymetric forecasting, visualization

1 Introduction

National Aeronautics and Space Administration (NASA) designed an Earth-observing satellite and successfully launched in July 1972 as the first Earth Resources Technology Satellite (ERTS-1), which was later known as Landsat 1. Since then another satellites (Landsats 2, 3, 4, 5, and 7) were successfully launched and operated. Landsat 6 was launched in September 1993 but failed to reach its orbit. Landsat 1, 2, and 3 operated in near-polar orbits at an altitude of 920 km with an 18-day repeat cycle. Landsat 4, 5, and 7 operated in orbits at an altitude of 750 km, lower then their predecessors, with a 16-day repeat cycle [6, 11, and 13]. Since 1972 all Landsat satellites have been acquiring many images, and therefore there are many multitemporal images for a specific area on earth available for many applications. In one year, 20 to 22 images of a certain (fixed) area will be available from one satellite. However, not all of the images of a certain area which were clear from cloud cover. Sometimes, in one year, no image available or only 1 image which is representative enough for further processing. The Landsat images can be processed to produce another images such as land cover images or bathymetric images which are important for land management, land conservation, coastal management, or bathymetric mapping. These specific images produced are known as thematic images (or simply digital thematic maps). There are many applications related to earth - either land or water - that can be derived from those earth observing satellite images.

Landsat 5 and 7 (also known as Landsat TM – Thematic Mapper) have 7 sensors where each sensor receives spectral radiance from earth in a specific wavelength λ (called band or channel). Band 1, 2, and 3 receive visible spectrum, i.e. blue, green, and red respectively. Band 4, 5, and 7 receive infra-red spectrum, while band 6 receives thermal infrared spectrum. Each band was carefully designed for specific applications as shown in Table 1 below.

Table 1. Spectral bands and their specific applications [13]

Color	Band (μm)	Applications
Blue	0.45 – 0.52	Soil/vegetation discrimination, deciduous/ coniferous forest differentiation, and clear water bathymetry
Green	0.52 – 0.60	Growth/vigor indication for vegetation, sediment estimation, and turbid water bathymetry
Red	0.63 – 0.69	Crop classification, ferric iron detection, ice and snow mapping
Near Infrared (NIR)	0.76 – 0.90	Biomass surveys, water-body delineation
Shortwave Infrared (SWIR)	1.55 – 1.75	Vegetation moisture, snow-cloud differentiation
Shortwave Infrared (SWIR)	2.08 – 2.35	Hydrothermal mapping, rock/soil type discrimination for mineral and petroleum geology
Thermal Infrared (TIR)	10.4 – 12.5	Thermal mapping, plant stress, urban/non urban land-use differentiation

Field measurements for *ground truth*, i.e. cross-checking between the digital numbers (pixel values) of satellite images and real field data, were usually conducted at different times. Normally, field measurements were conducted after processing the images which were acquired several days, weeks, months, or years in advance. Although the field data was not actually taken at the time when the image be acquired, the field measurements data can still be used (representative) whenever the parameters of study area is relatively not vary or no-changes between the satellite image acquired time and field measurement time [14].

Several researchs using satellite images for either clear water or turbid water bathymetry have been conducted. Hengel and Spitzer mentioned several algorithms for calculating water depth in coastal zone using satellite images developed by Lyzenga, Parades and Sparo, and Spitzer and Dirks. According to Lyzenga, Parades and Sparo, and Spitzer and Dirks, the water depth can be written as a linear combination of logarithms of the radiances [1,9]. Baban, Benny and Dawson, and Stove have also developed regression techniques for water depth calculation. All the techniques for bathymetry calculation considered spectral radiance of water body's characteristics as parameters, i.e. water clarity, depth, attenuation, sea-floor reflectance (if any), and suspension solids scatters [2, 5, 8, 10, and 12].

2 Methods

2.1 Study Area

The study area is located at the coastal zone, southern part of Papua Province, Indonesia, west of Papua New Guinea and north of Australia (Figure 1 - inset). The area boundary is 4°38'0" South, 136°36'0" East – 5°10'0" South, 137°21'21" East. In Universal Transverse Mercator (UTM), it is in Zone 53

South, (677996E, 9487669N) – (758876E, 9428089N). The area is therefore 59.6 km (north to south) by 80.9 km (west to east) or 4,820 km^2.

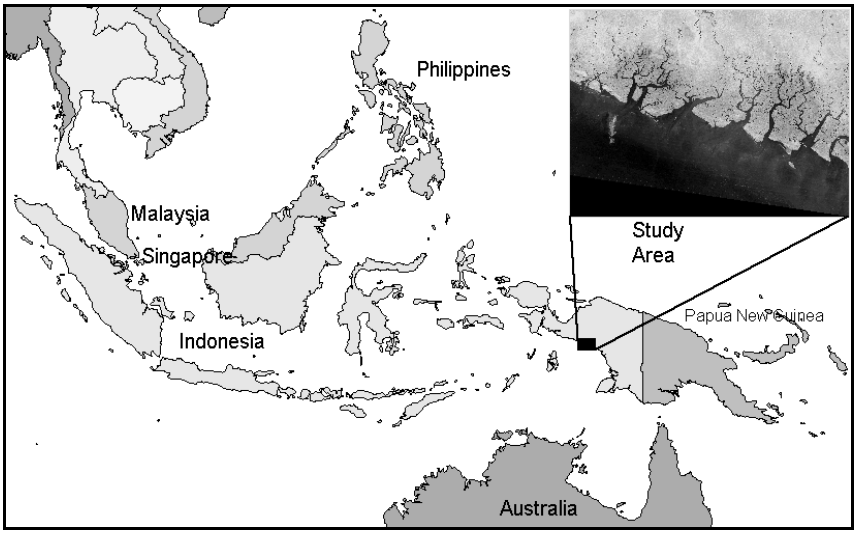

Figure 1 Study area

The area selected for the study is approximately 45% water (sea) and 55% non-water (mostly covered by vegetation/mangrove). The study area covers 6 estuaries, from west to east: Kamora, Tipoeka, Ajkwa, Minajerwi, Mawati, and Otokwa. The rivers of these estuaries are: Kamora, Wania, Tipoeka, Ajkwa, Minajerwi, Mawati, and Otokwa. Two of these rivers/estuaries, Ajkwa and Mawati, produce more sediments than the other, and therefore this study area is considered as a dynamic one and a good example for bathymetric forecasting study [14].

2.2. Data Set

For this study, 4 Landsat satellite images over study area (path/row - 103/63) were selected by considering the cloud coverage condition. The images were acquired May 1988, February 1991, November 1993, December 1996, and January 1999. Each image has 7 bands/layers, except for the image of year 1991 which has 6 bands/layers (band-6 is not available). The spatial resolution of Landsat image is 30x30 m for each pixel; this gives a raster image with 1986 rows and 2696 columns [6, 11, and 13]. Each image is in gray-scale format, which means that each pixel value range is 0 – 255 (for 8-bit unsigned). Value 0 is the darkest intensity (black) and value 255 is the brightest intensity (white). Figure 2a, b, c, and d are gray scale images with blue gradation color. For bathymetry study, the images were selected to produce images of water body area only. This area of interest contains 1,990,966 pixels (Figure 2).

Field depth data for 1990 were sampled at 7 locations (n = 7), for 1997 at 19 locations (n = 19), and for 1998 at 340 locations (n = 340); where n is number of samples. Samples in 1998 is much greater than the previous years, because this measurement were planned to be used as *ground truth* with the nearest acquired images [14].

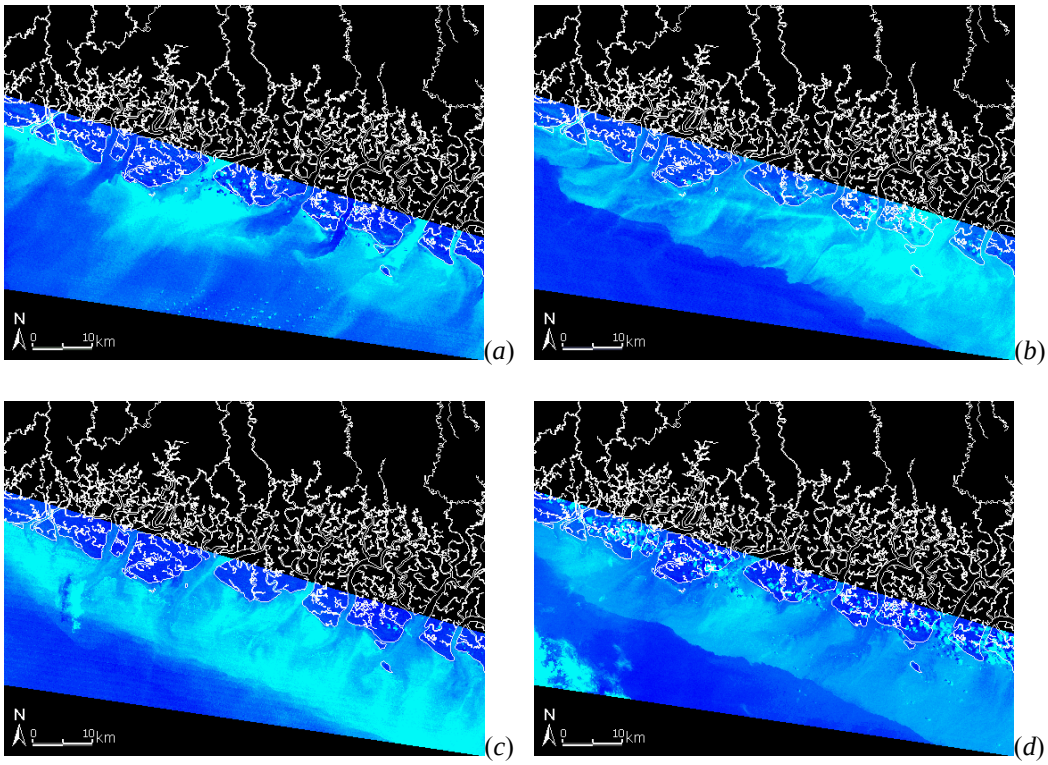

Figure 2 Colored/gray-scaled band-2 images – 1988(a), 1991(b), 1996(c), and 1999(d)

2.3. Approach

2.3.1. Digital number and field data relations

Bouguer-Lamber law showed that the intensity of electromagnetic spectrum varies with depth of water body. The formula for this law is $I=I_o \exp(-\kappa z)$ where I_o is the intensity at the surface, z is the depth, and κ is called the absorption coefficient. For turbid-water the maximum transmission is at about wavelength 0.575 μm (the color reflectance of water body is yellowish) [3, 4, and 7].

Each pixel of the Landsat images has 3 values, i.e. 2 for coordinates (East and North in UTM) and 1 for the spectral reflectance of the objects on earth surface (as digital number – DN). One set of Landsat image has 7 layers representing 7 bands, however for turbid-water bathymetry in this study, only one layer (band-2 or green) were utilized since the wavelength range covers the wavelength of yellow [14].

The field data measurements were conducted to get the real depth at the sampling locations. The field data will then be related to the digital number of band-2 Landsat images. The regressions of the four Landsat images and the field data produced 4 time series (layers) of bathymetry in 1988, 1991, 1996, and 1999. All layer formed a raster formatted database. Since the information were based on pixels of the images, the spatial analysis can be made as small as 30x30 m area which equals to the area of one pixel.

2.3.2 Cubic raster database

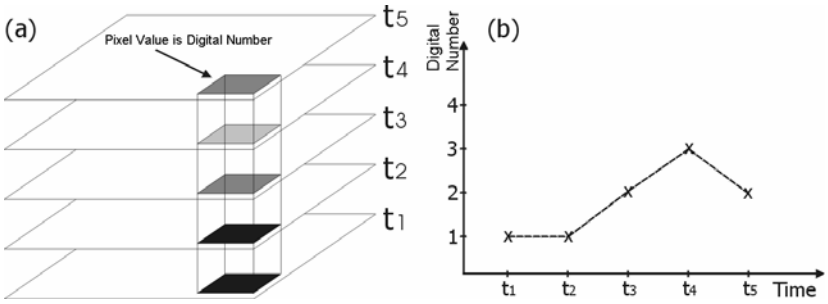

Figure 3 (a) Pixel values in four time series (layers), and (b) plot of digital number vs time for each pixel

Four layers of bathymetry were arranged and formed a cubic raster database (see Figure 3a). Each layer is a 2 dimension plane which represents one time, and the vertical axis is the third dimension, i.e. time. From every single pixel in one location in the database, one equation can be generated (Figure 3b). This means there will be more than 1.5 million equations. In this study, two equations (linear and quadratic regressions) will be used. Each equation tells the bathymetric characteristics (dynamics) of the 30mx30m area.

Linear regression $y = a_0 + a_1x$ has 2 constants, and quadratic regression $y = a_0 + a_1x + a_2x^2$ has 3 constants; where y is the depth of field measurement and x is the time of the image acquired. Standard error of estimation for linear regression has one value (constant) and for quadratic regressions has one value (constant). There are totally 7 constants. Each type of the constant can be treated as a spatial data and be arranged in one layer. So, there will be another cubic raster database containing 7 layers (values of constants) [14]. The unit of the constant was selected to be in range 0 – 255, because each pixel value used in this study was formatted in 8-bit unsigned. The selected format for this database is Band Sequential (BSQ) which is easily read and converted to other format.

2.3.3. Forecasting

In order to forecast the depth in a certain year, a layer will be generated from data in the cubic raster database containing the constants of the regressions. This layer may be appended or inserted into the bathymetry layers or treated as a free single layer. The bathymetric forecasting may use linear or the quadratic regression models [14]. By considering the standard error of estimation in both linear regression and quadratic regression models, user may use linear regression for certain areas and use quadratic regression for the rest. A user may generate forecasting images from the cubic raster database containing 7 layers (constants). Each generation will produce one image for one time (year). Therefore, for 5 forward forecasting images (for example, year 2000 to 2004), there will be 5 times of generations. These generations can be programmed for automatic calculation. The user just provides the forecasting unit of time needed, and type of forecast either forward or backward.

2.3.4. Animation

By the availability of images of original data, backward forecasting, and forward forecasting, the time series images showing bathymetric condition for the area study is available. In order to give more

impressive visualization, those time series images can be arranged as an animation image. Animated gif is selected for this animation for its simplicity and is easily viewed in windows explorer or in a browser (if inserted in web page).

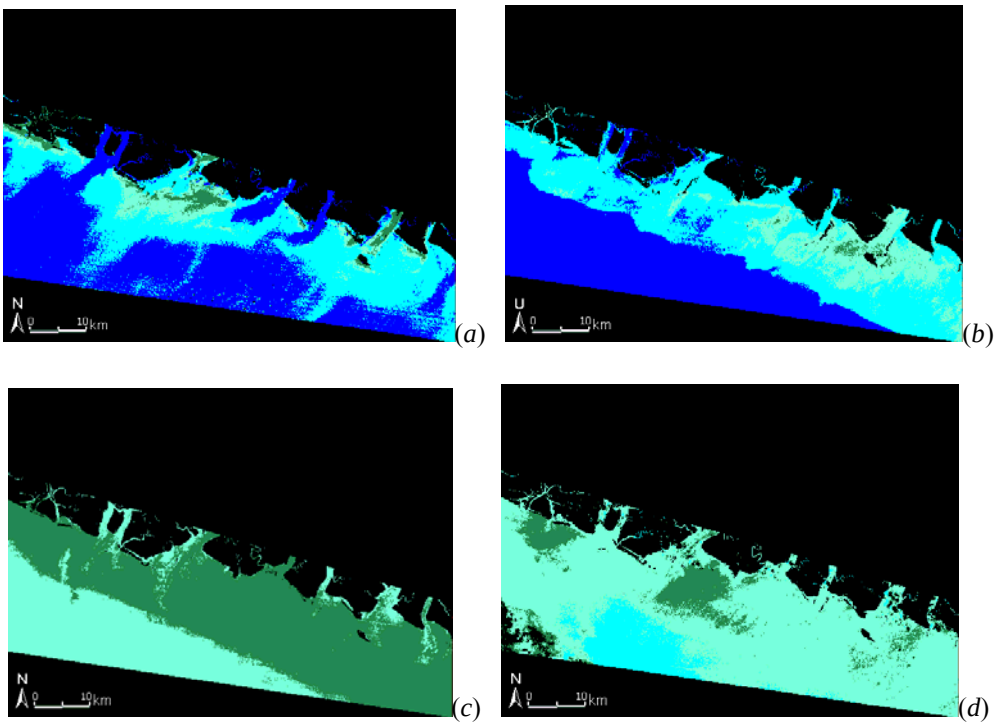

Figure 4 Bathymetry images in 1988(a), 1991(b), 1996(c), and 1999(d)

3. Results and Discussion

The results are better viewed in colors, since the colors provide information about the bathymetry characteristics from 1988 to 1999 over the study area. Figure 4 a, b, c, and d show the bathymetry for 1988, 1991, 1996, and 1999 respectively. There are four color for the depth classes. Green for depth $\leq$ 3 m, light green for depth 3-5 m, cyan for depth 5-10 m, and blue for depth > 10 m. The images of 1996 and 1999 show a dynamic change that is not easy to be explain. The limited field data may be one source of result inaccuracy or there were activities that disturbed the natural process in a coastal zone.

Figure 5 shows 36 samples of linear regression (5a) and quadratic regression (5b) equations. The trends in linear model are decreasing in depth. The trends in quadratic can be divided into two groups. The first group is decreasing in depth, and the second one is increasing and then decreasing in depth. The second group is possible and may happen in the nature.

Figure 6 shows the negative values a_1 (*slope*) of linear regression model. The values of slope were classified into 3 classes and were represented in 3 different colors, yellow (0-0.5), cyan (0.5-1), and

magenta (>1). From the colors in the spatial image, a user can easily interpret the pattern of changes in depth from 1988 to 1999.

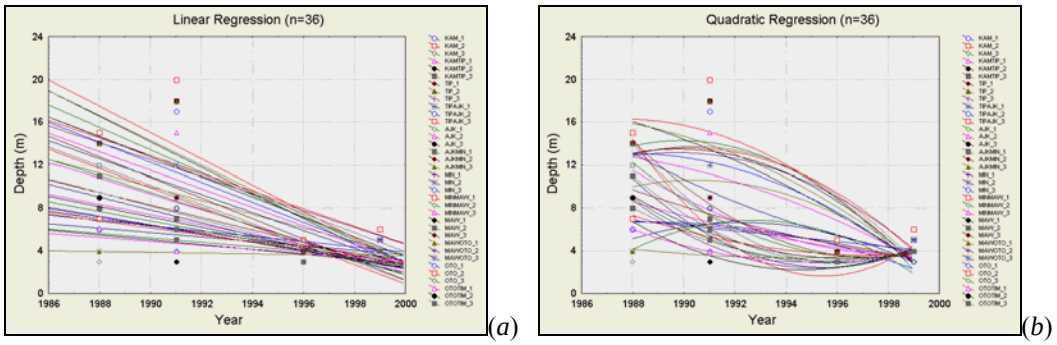

Figure 5 Linear regression samples (a), Quadratic regression samples (b)

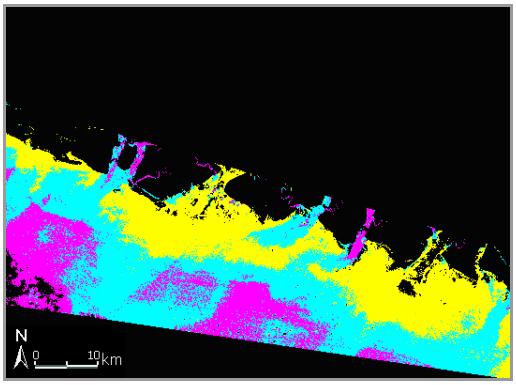

Figure 6 Plot of linear regression constant a_1 (slope)

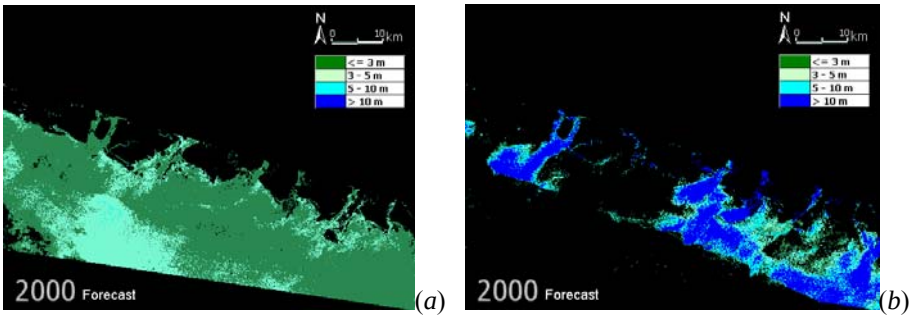

Figure 7 Forecast bathymetry - linear regression (a), Forecast bathymetry - quadratic regression (b)

Figure 7a shows the forecast bathymetry for year 2000 using linear regression, and Figure 7b shows the forecast bathymetry for year 2000 using quadratic regression. The water depth was classified into 4 classes with 4 different colors. Green for depth $\leq$ 3 m, light green for depth 3-5 m, cyan for depth 5-10 m, and blue for depth > 10 m. The images of Figure 7a and 7b were formatted in

animated gif, but unfortunately the user can not see the animation in this paper. Figure 8a shows the time series of linear regression images, and Figure 8b shows the time series of quadratic regression images, ready to be converted to animated gif format.

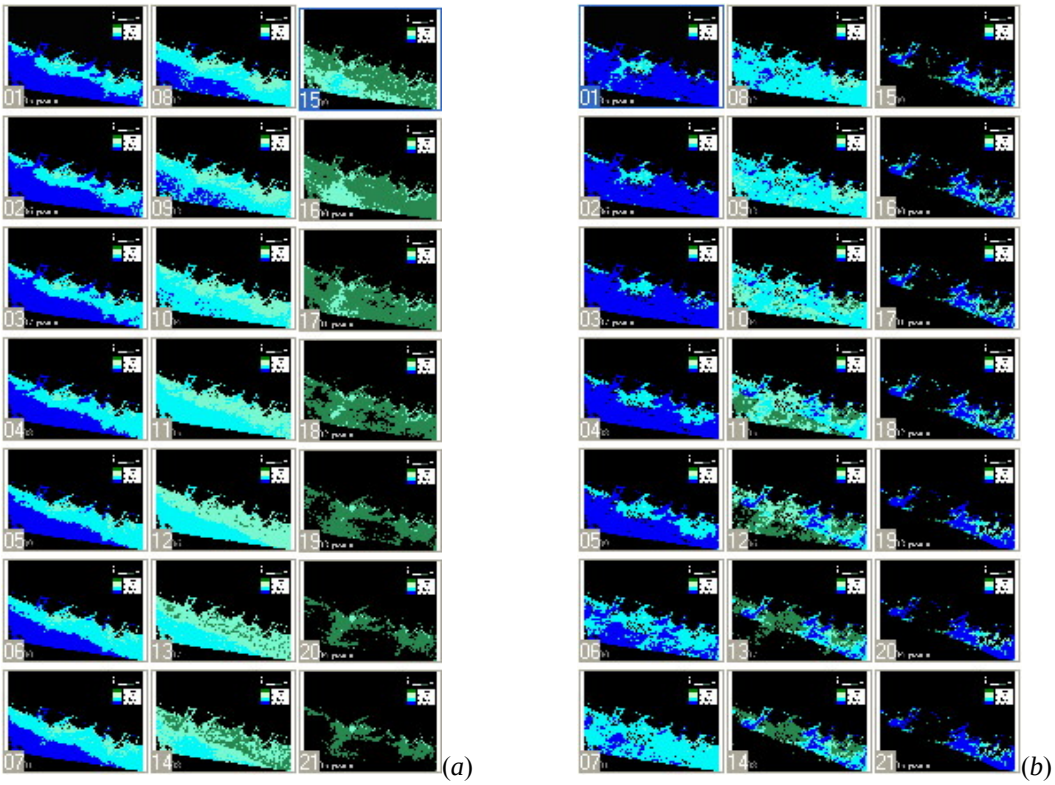

Figure 8 Time series images - linear regression (a), Time series images - quadratic regression (b)

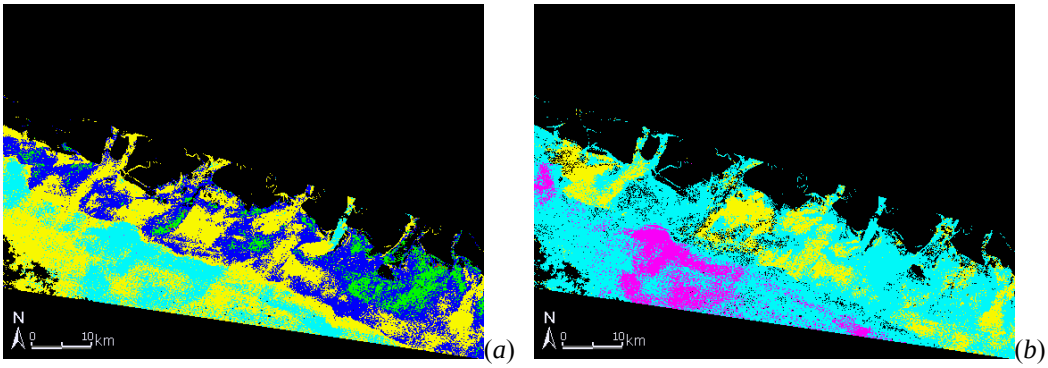

Figure 9 Standard error for linear regression (a), Standard error for quadratic regression (b)

The standard error of estimation quantifies the spread of the data around the regression line. The standard error of estimation values for linear (Figure 9a) and quadratic (Figure 9b) regressions were

classified into 6 classes with 6 different colors as follow: red (1-5), green (6-10), blue (11-20), yellow (21-50), cyan (51-100), and magenta (101–255). The unit is in decimeter.

By visual observation of Figures 9a and 9b, the standard errors with lower values (blue, green, and yellow - near the shoreline) can easily be detected in Figure 9a. This tells that the estimation using linear model is more accurate than the quadratic model. The user may then decide which certain area uses linear model and the rest uses quadratic model. This combined linear and quadratic models becomes a hybrid regression model for bathymetric forecasting.

4. Conclusions

By using multilayer spatial data which was arranged in cubic raster database and saved in Band Sequential (BSQ) format, it is possible to generate another cubic raster database containing constants or forecasting values. The spatial image showing values or constant(s) of an equation may open the way of observing the spatial data. This way, the observer/user can evaluate the techniques used in forecasting using multilayer spatial images and the forecasting bathymetric values. He/she may then decide to plan for another detailed or advanced study in the area which shows less accurate in estimation or calculation.

Cubic raster database can be used to store multitemporal data (multilayer spatial images), forecasting data (forward extrapolation), historical data (backward extrapolation), interval or in-between data (interpolation), constants of the equations (e.g. regression) utilized in forecasting, as well as the standard errors or standard deviations. The new layer can be generated from the database to provide spatial information to be observed or interpreted by the user. In order to visualize the bathymetric change from time to time (in time series), all images can also be animated.

References

1. Baban, S.M.J., The evaluation of different algorithms for bathymetric charting of lakes using Landsat imagery. International Journal of Remote Sensing. Vol 14, No 12, pp. 2263-2273. 1993.
2. Bagheri, S., Stein, M., and R. Dios., Utility of hyperspectral data for bathymetric mapping in a turbid estuary. International Journal of Remote Sensing. Vol 19, No 6, pp. 1179-1188. 1998.
3. Beer, T., Environmental Oceanography. 2/ed. CRC Press, Boca Raton, Florida. 1997.
4. Bemmet, A.J., and D.G. Troost, Environment and development in coastal regions and in small islands. Coastal Management Sourcebooks 3. http://www.unesco. org/csi. 2000.
5. Bierwirth, P.N., Lee, T. and R.V. Burne, Shallow Sea-Floor Reflectance and Water Depth Derived by Unmixing Multispectral Imagery, on 1st Thematic Conf. on Remote Sensing for Marine and Coastal Environments, 1992.
6. Byrnes, R., Landsat 4/5 Operations to End. News Release. U.S. Dept of Interior U.S. Geological Survey, http://www.usgs.gov/ article.asp?id= 472. Accessed May, 2001.
7. Forster, B., Baide, X., and S. Xingwai, Modelling suspended particle distribution in near coastal waters using satellite remotely-sensed data. Intel J. of Remote Sensing. Vol15, No6, pp.1207-1219, 1994.
8. Geeorge, D.G., Bathymetric mapping using a Compact Airborne Spectrographic Imager (CASI). International Journal of Remote Sensing. Vol 18, No 10, pp. 2067-2071. 1997.
9. Hengel, W. Van and D. Spitzer, Multitemporal water depth mapping by means of Landsat TM. International Journal of Remote Sensing. Vol 12, No 4, pp. 703-712. 1991.

10. Ibrahim, M. and A.P. Cracknell, Bathymetry using Landsat MSS data of Penang Island in Malaysia. International Journal of Remote Sensing. Vol 11, No 4, pp. 557-559. 1990.
11. Laurer, D.T., Morain, S.A., and V.V. Salomonson, The Landsat Program: Its Origins, Evolution, and Impacts. Photogrammetric Engineering & Remote Sensing. Vol 63, No 7, pp. 831-838. 1997.
12. Lee, K.S., Kim, T.H., Yun, Y.S., and S.M. Shin, Spectral Characteristics of Shallow Turbid Water near Shoreline on Inter-tidal Flat. Korean J. of Remote Sensing. Vol17, No2, pp. 131-139. 2001.
13. Mika, A.M., Three Decades of Landsat Instruments. Photogrammetric Engineering & Remote Sensing. Vol 63, No 7, pp. 839-852. 1997
14. Paryono, P., Digital Image Modelling for Coastal Biogeophysical Environment Changing using Landsat Thematic Mapper Images. Ph.D. Dissertation, Gadjah Mada University, 2003.